Egyptian Journal of Aquatic Biology & Fisheries
Zoology Department, Faculty of Science,
Ain Shams University, Cairo, Egypt.
ISSN 1110 – 6131
Vol. 26(6): 595 – 617 (2022)
www.ejabf.journals.ekb.eg

Determination of Potentially Toxic Metals in Mangrove Trees and Associated Sediments Along Saudi Red Sea Coast

Zaki M. Al-Hasawi
Biological Sciences Department, Faculty of Science, King Abdulaziz University, P.O. 80203, Jeddah 21589, Saudi Arabia
zalhasawy@kau.edu.sa

ARTICLE INFO

Article History:
Received: Dec. 5, 2022
Accepted: Dec. 12, 2022
Online: Dec. 16, 2022

Keywords:
Potentially toxic elements (PTEs),
Ecological Risk Assessment,
BAFs,
Sediment-mangrove ecosystem,
Red Sea coastline

ABSTRACT

Monitoring and surveillance of mangrove ecosystem are highly significant, especially in the coastal zones; which receive heavy metal pollutants from the anthropogenic activities. Thus, the determination of toxic metals (Zn, Mn, Cu, Cr, Ni, Pb, Co and Hg) in *Avicennia marina* ecosystem along the Saudi Arabian Red Sea coast was addressed. to evaluate the level of concentration of the investigated heavy metals. To evaluate the level of concentration of the investigated heavy metals, surface sediment samples as well as roots and leaves were collected from Al-Birk, Almazilif, Jeddah, Zahban, Thuwal Island, Rabigh-I, Rabigh-II, Masturah, Yanbu, and Duba between March and June 2021. The following sequential average concentrations of several trace elements were determined: Mn (258.16±127.06μg g^{-1}) > Cr (51.48 ±16.01 μg g^{-1}) > Zn (39.34 ±17.82 μg g^{-1}) > Ni (30.42±17.88 μg g^{-1}) > Cu (29.51 ±13.62 μg g^{-1}) > Co (11.31±6.95 μg g^{-1}) > Hg (0.98 ±0.20 μg g^{-1}), respectively. While, the higher PETs of Zn (84.19 μg g^{-1}), Mn (495.20 μg g^{-1}), Ni (67.08 μg g^{-1}), and Co (27.41 μg g^{-1}) were greater at the Rabigh-II site. According to the Cd readings, 10% of the sites were moderately contaminated (Cd = 7), while 90% were highly contaminated (Cd = 14). Indices used in ecological risk assessments correlate with the I_{geo} index. Pb (0.61) > Cu (0.44) > Ni (0.33) > Cr (0.32) > Zn (0.31) > Mn (0.22) > Hg (0.15) > Co (0.11) was the descending average BAF for mangrove leaves, while Pb (0.31) > Ni (0.29) > Cu (0.26) > Hg (0.24) > Cr (0.21) > Zn (0.17) > Co (0.11) > Mn (0.11) was the descending average BAF for roots. This study demonstrated the possibility of developing a framework for managing the Red Sea coast of Saudi Arabia's coastal marine ecosystems.

INTRODUCTION

Mangrove trees or shrubby plants are dominating and distributing in the coastal intertidal zone of both tropical and subtropical regions. Mangroves are vital for many reasons, including carbon sequestration , seawater purification and protection from wind and waves **(Qi-juan *et al.*, 2021)**. Mangroves are sporadic in their distribution, confined channels and the interior sides of offshore islands; they are only found in low-energy, peaceful habitats such as bays **(Kumar, 2017)**. Mangrove forests can be found off the coasts of Farsan, Jazan, Qunfudhah, Al-Leith, and Jeddah in the west, and Dammam, Saihat, Qatif, and Safwa in the east, all the way to Ras Tanura. Due to urbanization, mangrove forests along the coasts of these cities are diminishing or disappearing. The Red Sea tidal area of Saudi Arabia is considered as a suitable zone to several different types of mangrove trees, the most common of which are *Avicenna marina* and *Rhizophora mucronate* **(El-Juhany *et al.*, 2009; Kumar, 2017)**.

Heavy metal pollutants have been produced due to rapid urbanization, especially with the continuous increase of industrial and agricultural effluent activities in coastal areas. These pollutants have flowed into the sea via runoff and direct discharges near the shore, severely damaging mangroves **(Tokatli, 2019; Jiang *et al.*, 2020; Ustaoğlu *et al.*, 2020; Sarker *et al.*, 2021)**.

Ecosystem contamination is on the rise and has become a concern on a global scale because of the permanent presence of harmful heavy metals in aquatic ecosystems and their widespread dissemination **(Yuan *et al.*, 2011, Mosa *et al.*, 2022)**. The world's continental shelf and coastal zones become contaminated via pollutants floating in the water and by those entering via effluents and runoffs on land. Therefore, upon sinking into the benthic sediment of the water, the natural status and wellbeing of the ecosystem could be affected **(Zhang *et al.*, 2017; Bakshi *et al.*, 2018)**. More recent efforts have focused on using multivariate statistical methods and indices, including the Pearson correlation index (PCI), principal components analysis (PCA), and cluster analysis (CA) to identify the origins and connections of heavy metals and collect more precise information on surface water quality **(Zhou *et al.*, 2007; Mustapha and Aris, 2012; Mustapha *et al.*, 2012; Kiymaz *et al.*, 2014; Muangthong, 2015)**.

The main objective of this research was to evaluate the levels of zinc, copper, manganese, nickel, lead, cadmium, chrome, and mercury in the mangrove surficial sediments and plants (leaves and roots). The enrichment factor (EF), contamination factor (CF), geo-accumulation index (*Igeo*), hazard index (HI), hazard quotient (HQ), and potential environmental dangers and toxicities to human health were utilized to assess the level of contamination in sediments. In addition, the study shed insight on the current condition of metal contamination in sediments and its accumulation inside the various compartments of mangrove trees.

MATERIALS AND METHODS

1. Investigated areas

The study area is approximately 1.840 kilometers of the Red Sea coastline located in Saudi Arabia, making up around 79% of the eastern part of the Red Sea basin. About 135 km^2 of the Red Sea's shoreline is covered with mangrove forests, providing a natural vegetative ecology **(Almahasheer *et al.*, 2016)**. The research area covered the entire length of the Saudi Arabian Red Sea coast, from Al-Birk in the south to Duba in the north, as shown in Table (1) and (Fig (1). Each sampling site's coordinates were geographically determined using a Global Positioning System (GPS; Garmin Etrex 10).

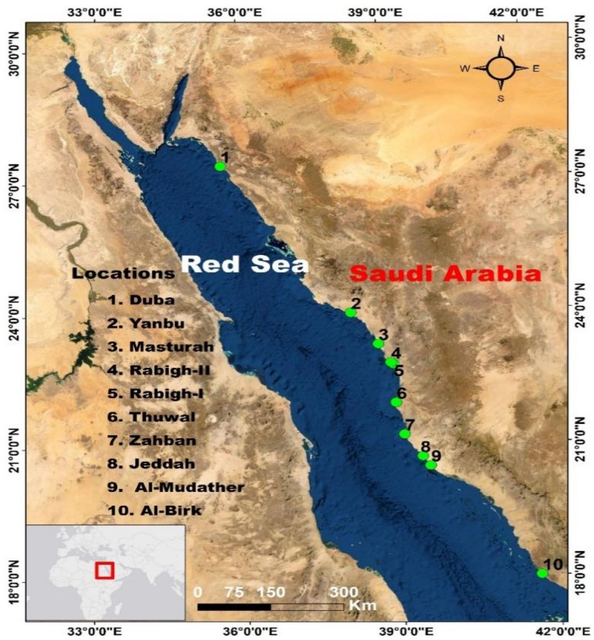

Fig. 1. The study area map showing the sampling sites along the western coast of the Red Sea , Saudi Arabia

The samples were collected between March and June 2021. Sediment samples and mangrove organs, such as aerial roots and leaves were collected. Table (1) and Fig. (1) show the location of the selected sites and their GIS information.

Table 1. Tabulated latitudes and longitudes of the sampling sites

	Name	Latitude	Longitude	Characterized by
1	Duba	27°25'38.47"N	35°36'5.57"E	Inland lagoon away from any activities
2	Yanbu	23°59'0.80"N	38° 4'47.27"E	Located in an arid topography that is devoid of important estuaries and is considered as one of the most active cities along the Saudi coast of the Red Sea
3	Masturah	23°19'45.49"N	38°41'15.70"E	Occupied at end of Wadis
4	Rabigh-II	22°16′54.42″N	39◦5′6.12″E	Occupied the center of it adjacent to petro-chemical factory and oil shipping
5	Rabigh-I	21°16'8.27"N	39°7'33.13"E	at the end of Sharm
6	Thuwal	22°16'12.83"N	39° 1'7.07"E	Human accomplishments and modern coastal progress
7	Zahban	21°48'4.02"N	39° 0'46.96"E	Human Activity
8	Jedahh	21°31'28.29"N	39° 3'47.81"E	Near the sewage sludge treatment station
9	Almazilif	18°38'1.62"N	41°12'43.18"E	Many of aquaculture and mangrove patches
10	Al-Birk	18° 0' 55.90" N	41° 39' 14.40" E	Laid out at end of Wadis and embodied the back reef characterized with huge stands of mangrove swamps

2. Sampling proceedings and trace elements analysis

Three subsamples of sediments of about 500g were collected from the rhizosphere zone of mangrove trees at each site and mixed in a polyvinyl chloride (PVC) core to create a bulk composite sample.

The collected sediment samples were transported to the lab in plastic bags and air-dried to a constant weight. Standardized procedures **(Jackson, 2005; Piper, 2017; Dane & Topp, 2020; Sparks *et al.*, 2020)** were used to characterize the sediments' physico-chemical properties.

The total amounts of trace elements in grey mangrove leaf and root tissues were evaluated by collecting three leaves from each of three opposite branches to make composite sample. The heavy metals were measured by iCAPTM 7000 Plus Series ICP-OES (Thermo ScientificTM, USA) to determine the values of Zn, Cu, Mn, Ni, Cr, Co, Pb, and Hg levels according to methods of **Bettinelli *et al.* (2000)**.

Conductivity/TDS/Salinity/Temperature meters were used to measure the electrical conductivity (ECs) of a sediment/water extract at a ratio of 1:2.5. **(Jackson, 2005)**. HANNA HI2221 Benchtop pH/mV meter was used to measure the pH of sediment reaction in suspensions of sediment/water at a ratio of 1:2.5 according to the method of **Jackson (2005)**.

3. Assessment of ecological risk indices

Based on the calculation of the following factors, an assessment of the pollution of the grey mangrove-sediment ecosystem was recognized:

Contamination factor (Cf)

Pollution and environmental contamination effects are reflected in the contamination factor (Cf), which is calculated by dividing the concentration of each trace metal in the sediment background by itself. The following facts are established:

$$C_f = \frac{C_s}{C_b} \qquad (1)$$

Where,

is the concentration of trace metals in the sediments

is the concentration of trace metals in the sediments as a reference value **(Turekian & Wedepohl, 1961)**.

To classify the varying contamination factor ranges, **Håkanson (1980)** was used as a reference, where,

Cf < 1 denotes low contamination;

1 ≤ Cf < 3 indicates moderate contamination;

3 ≤ Cf < 6 can be reflected as below the higher-level contamination,

and Cf ≥ 6 is a category that can indicate high levels of contamination.

The pollution load index (PLI)

The integrated pollution load index (PLI) is considered as the root of PTEs-contamination factors summation following the equation:

$$PLI = \sqrt[n]{CF1 \ x \ CF2 \ x \ \ldots\ldots CFn} \qquad (2)$$

Geo-accumulation index (I_{geo})

Müller (1969) postulated the geo-accumulation index (I_{geo}), which is determined by the following formula:

$$\boldsymbol{I_{geo} = log_2\left[\frac{C_n}{1.5 . B_n}\right]} \qquad (3)$$

Where, C_n is the concentration of trace metal (n) in sediment, and *Bn* is the geochemical background value in the shale, as reported by **Turekian and Wedepohl (1961)**. Subsequently, seven standards were established according to **Müller (1969)**.

At *Igeo* values of 0, 1, 1-2, 2-3, 4-5, and > 5, the levels of contamination were categorized into: uncontaminated, uncontaminated to moderately contaminated, moderately contaminated, moderately contaminated, moderately contaminated to very contaminated. The potential for reference value variation owing to lithogenic inputs was accounted for by setting the constant at 1.5.

The degree of contamination (Cd)

It is assumed that the degree of contamination (Cd) is proportional to the sum of all contamination components; it was assessed with the succeeding formula:

$$\boldsymbol{Cd = \sum_{i=1}^{n} C_f^i} \qquad (4)$$

Where, if the Cd value is ≤ 7, the level of contamination would be minimal.

Cd levels between 7 and 14 are considered moderate.

If CD is between 14 and 28, then conspicuous levels of pollution are determined.

The extremely high concentrations of cadmium (Cd) are at or above 28 parts per billion.

Potential ecological risk index (E_r^i)

The potential ecological risk index (E_r^i) and potential toxicity index (RI) were calculated according **Håkanson (1980)**, using the following equation:

$$E_r^i = \boldsymbol{T_r^i \ x \ \frac{C_i}{C_0}} \qquad (5)$$

Where,

T_r^i is the hazardous response factor for a given trace metal (e.g., Zn, Pb, Mn, Cu, Ni = 5; Cr = 2 and Co, Hg = 40);

C_i is the concentration of that metal in the sediment, and

C_o is the background concentration of that metal.

Trace metal toxicity in sediments and subsequent environmental response were estimated using the potential toxicity response index (RI). Hence, the following formula is supposed to be the ecological risk index (RI):

$$\boldsymbol{RI} = \sum_{i=1}^{n} \boldsymbol{E_r^i} \qquad (\boldsymbol{6})$$

Where,

RI criteria by trace metals are assumed by **Håkanson (1980)**;

E_r^i < 40 indicates low risk (LR), and

$40 \leq E_r^i < 80$ indicates moderate risk (MR).

Potential toxicity index (RI) was classified into four levels as the follows:

RI < 150: low risk (LR);

150 ≤ RI < 300: moderate risk (MR);

300 ≤ RI < 600: considerable risk (CR), and

600 ≤ RI: very high risk (VHR).

4. Biological accumulation factor (BAF)

The capability of the plant to intake varied trace metals from rhizosphere sediment to various tissues (leaves, areal roots, canopy and fruits) was expressed as a biological accumulation factor (BAF) that was calculated as follows:

$$\mathbf{BAF}_{leaf} = \boldsymbol{C_{leaf}}/\boldsymbol{C}_{sediment} \qquad (7)$$

$$\mathbf{BAF}_{root} = \boldsymbol{C_{root}}/\boldsymbol{C}_{sediment} \qquad (8)$$

Where,

$\boldsymbol{C}_{leaf}$ and $\boldsymbol{Cl}_{root}$ is the content of trace metal in leaf and areal root tissues, while $\boldsymbol{C}_{sediment}$ is the content of trace metal in the surrounding sediment.

Translocation factor (TF)

The translocation factor (TF) for estimated PTEs concentration is calculated via the following equation.

$$\mathbf{TF}_{leaf} = \boldsymbol{C_{leaf}}/\boldsymbol{C}_{roots} \qquad (9)$$

Where, $\boldsymbol{C_{leaf}}$ and $\boldsymbol{C}_{roots}$ are the PTEs content in the leaf and root tissues, respectively.

6. Statistical analysis

A descriptive statistical analysis of the relevant variables was performed using SPSS (version 24.0). In addition, the PTEs concentration in sediment, leaf, and areal root samples was correlated to their physico- chemical parameters using Pearson's correlation coefficient. A principal component analysis (PCA) using the factor extraction technique for statistical purposes was performed. After applying Varimax rotation, the eigenvalue was determined for a value greater than 0.60.

RESULTS AND DISCUSSION

The particle size distribution in sediments is a crucial factor in determining the source material and lithogenic pathways of sediment deposition **(Ali *et al.*, 1987)**.

In the present investigation, Table (2) reveals that 97.55% of sediments were constituted of sand, with percentages ranging from 95.43% at the Yanbu site to 99.00% at

Masturah. While, the mud proportion varied from 1.00% to 4.57% at the Masturah and Yanbu sites, respectively; the range was between 1.00% and 4.57%. (Average of 1.16).

Sandy, siliceous, *hyperthermic*, *aquic Torripsamments* is the final texture defined for the selected locations. Multiple causes including lithogenic origin, parent material character, urban encroachment, and coastal shoreline degradation in the study area are likely liable for the existence of fine particles in nearly all sediment samples. The variation in marine sediment grain size can be influenced by several processes, viz. sedimentation and sediment transport **(Håkanson, 1980)**.

Table 2. Surface sediments characteristics along the coast of Saudi Arabia Red Sea

Location	**Particle size distribution**		**Texture type**	**pH**	**EC (dSm^{-1})**	**$CaCO_3$%**	**SOC %**
	Sand	**Mud**	Sandy				
Duba	97.34	2.66	Sandy	8.08	9.90	15.70	2.00
Yanbu	95.43	4.57	Sandy	7.76	13.09	16.02	2.60
Masturah	99.00	1.00	Sandy	8.03	23.09	19.00	4.50
Rabigh-II	95.78	4.22	Sandy	7.45	8.90	18.40	1.87
Rabigh-I	97.43	2.57	Sandy	7.81	6.90	21.90	2.47
Thuwal	98.00	2.00	Sandy	8.25	13.98	17.90	3.09
Zahban	98.40	1.60	Sandy	7.35	18.90	19.00	1.52
Jeddah	98.42	1.58	Sandy	7.78	7.90	15.90	1.05
Almazilif	97.38	2.62	Sandy	8.06	17.98	20.20	1.07
Al-Birk	98.34	1.66	Sandy	7.78	7.31	13.20	2.03
Descriptive statistics							
Min.	95.43	1.00		7.35	6.90	13.20	1.05
Max.	99.00	4.57		8.25	23.09	21.90	4.50
Average	97.55	2.45		7.84	12.80	17.72	2.22
St. dev.	1.16	1.16		0.28	5.62	2.54	1.03
Skewness	-0.91	0.91		-0.41	0.70	-0.16	1.15
Kurtosis	-0.003	-0.003		-0.39	-0.76	-0.14	1.77

Numerous studies demonstrated that mangrove ecosystems can act as a primary heavy metal sink by increasing the deposition of suspended solids and slowing water movement **(Spencer *et al.* 2003)**. In addition, the sediments' physical, chemical, and biological processes led to the constant remobilization of heavy metals in water bodies **(Sanders *et al.* 2012)**. Most of the sediment samples analyzed had alkaline pH levels, ranging from 7.35 to 8.25 at Zahban and Thuwal Island, respectively (Average: 7.84±0.28). The conductivity readings varied from 6.90 dSm^{-1} at Rabigh-I to 23.09 dSm^{-1} at Masturah (Mean: 12.80 ± 5.62 dSm^{-1}). Large amounts of rain fell on some mangrove regions of the Arabian Gulf, causing the conductivity to drop and accounting for the observed variances in conductivity. Organic content in mangrove silt may have been assimilated from terrigenous sources or through the decomposition of animals and plants **(Kristensen *et al.*, 2008)**. Sediment organic matter concentration ranged from 1.05 in

Jeddah to 4.50% at Masturah, with a mean value of 2.22% ±1.03. Surface sediment OM levels in the Arabian Gulf mangroves were notably lower than the global average of 7.9% in estuarine tropical mangrove ecosystems **(Rogers *et al.*, 2013)**. Fast tidal export cause lower level values, which could bring organic molecules produced inland to the coast, which could be responsible for the lower amounts observed (Rogers *et al.*, 2013).

However, coarse grains derived from terrigenous sediments, which are negatively charged, can inhibit the absorption of organic compounds, leading to lower results **(Kumar *et al.*, 2016)**. The present investigation found that the carbonate concentration of sediments varied from 13.20% at Al-Birk to 21.90% at Rabigh-I, with an average of 17.72% 2.54. Most of the carbonate in this sample came from terrigenous materials and biological origins on land.

Spatial distribution of PTEs concentrations in mangrove sediments

Most PTEs readings were larger in magnitude at Rabigh locations. At Rabigh-II, the highest amounts of Zn (84.19 µg g^{-1}), Mn (495.20µg g^{-1}), Ni (67.08 µg g^{-1}), and Co (27.41 µg g^{-1}) were recorded.

Zn, Cu, Mn, Ni, Pb, Cr, Cd, and Hg recorded concentrations between 19.60-39.34, 15.78-52.21, 85.80- 495.20, 19.00- 67.08, 4.07-10.04, 28.90-76.79, 1.78-27.41, and 0.65-1.20 µg g^{-1}, respectively, (Fig. 2, 3). Following is a list of trace elements in descending order of their mean concentrations: 258.16±127.06 for Mn > 51.48 ± 16.01 for Cr > 39.34 ±17.82 for Zn > 30.42±17.88 for Ni > 29.51±13.62for Cu > 11.31±6.95 for Co> 0.98± 0.20 for Hg. Higher PTE values were observed at Rabigh locations. At Rabigh-II, the highest amounts of Zn (84.19 µg g^{-1}), Mn (495.20µg g^{-1}), Ni (67.08 µg g^{-1}) and Co (27.41 µg g^{-1}) were registered.

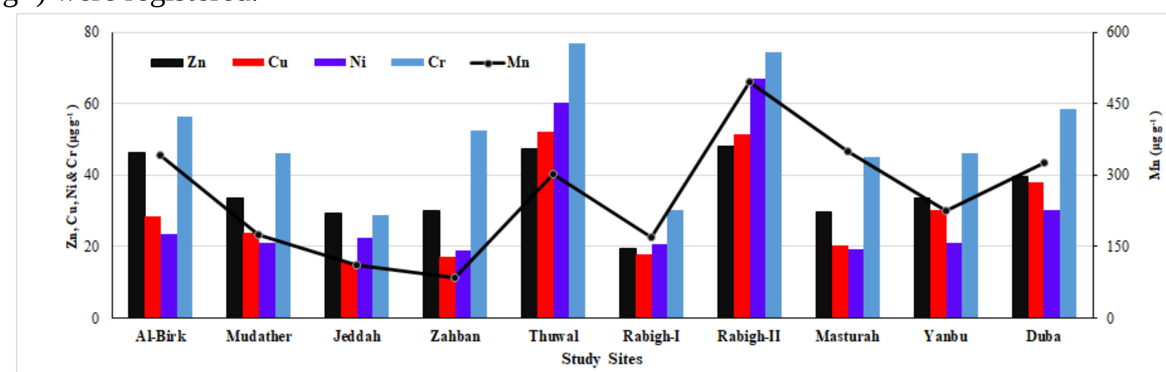

Fig. 2. Trace metals concentrations (µg g^{-1})(Zn, Cu, Ni, Cr., Mn) in sediments of the grey mangrove ecosystem at study sites

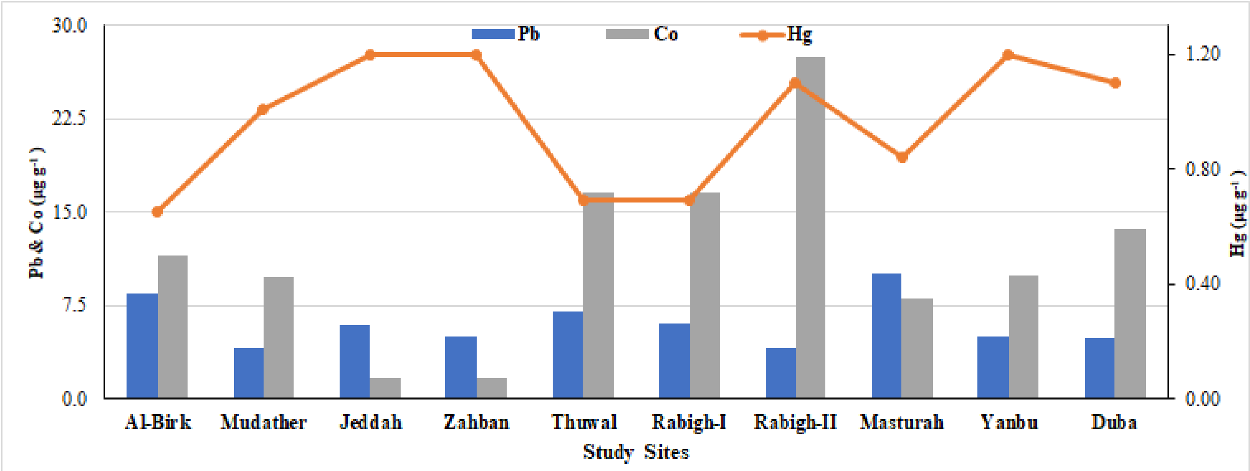

Fig. 3. Trace metals concentrations (µg g^{-1}) (Pb,Co,Hg) in sediments of the grey mangrove ecosystem at study sites

Stimulatingly, most PTEs concentrations were recorded at locations subjected to different urbanization features, such as aquaculture farming waste, oil transport harbors, cement plants, power generation and desalination stations **(Abohassan, 2013; Alzaharani *et al.*, 2018; Alharbi *et al.*, 2019)**.

PTEs were found in high enough quantities in areas exposed to a variety of urbanization factors, including oil transport harbors, a cement industry, a power generating and desalinization station and the waste from aquaculture farms **(Abohassan, 2013; Alzaharani *et al.*, 2018; Alharbi *et al.*, 2019; Al-Hasawi *et al.*, 2022)**.

As shown in Table (3), the results are compared with different published studies in varied national and international countries, for example, USEPA **(Beyer, 1990)**, Panama **(Guzmán & Jiménez, 1992)**, Singapore **(Cuong *et al.*, 2005)**, China **(Qiu *et al.*, 2011)**, Saudi Arabia **(Abohassan, 2013; Alharbi & El-Sorogy, 2017; Al-Zaharani *et al.*, 2018; Alharbi *et al.*, 2019)**, Egypt **(El-Said & Youssef, 2013)** and Bangladesh **(Kumar *et al.*, 2016)**.

Table (3) displays the results of a comparison with studies conducted in other countries, including Singapore **(Beyer, 1990)**, Washington D.C. **(Cuong *et al.*, 2005)**, China **(Qiu *et al.*, 2011)**, Saudi Arabia **(Abohassan, 2013; Alharbi & El-Sorogy, 2017; Al-Zaharani *et al.*, 2018; Alharbi *et al.*, 2019)**, Egypt **(El-Said & Youssef, 2013)** and Bangladesh **(Kumar *et al.*, 2016)**.

Table 3. Comparison of PTE contents (µg g^{-1}) in surface sediments with national and international countries.

Location	PTE contents (µg g^{-1}) in surface sediments								Reference
	Zn	Cu	Mn	Ni	Pb	Cr	Co	Hg	
Min.	19.60	15.78	85.80	19.00	4.07	28.90	1.78	0.65	Current study
Max.	84.19	52.21	495.2	67.08	10.04	76.79	27.41	1.20	
Average	**39.34**	**29.51**	**258.2**	**30.42**	**6.09**	**51.48**	**11.31**	**0.98**	
UCC	71	25	600	50	16	85	17	0.05	Taylor & McLennan, 1985
Arabian Gulf, Saudi Arabia	52.7	182.9	113.9	75.10	5.36	51.03	4.75	0.80	Alharbi & El-Sorogy, 2017
Red Sea, Saudi Arabia	--	22.87	--	21.11	3.82	46.11	--	--	Alzaharani *et al.*, 2018
Bangladesh	74.09	44.69	740.9	207.3	25.61	52.87	17.56	ND	Kumar *et al.*, 2016
Red Sea, Egypt	--	49.9	133	28.1	19.0	--	6.7	--	El-Said & Youssef, 2013
China	57	18	ND	ND	19.0	40	--	0.08	Qiu *et al.*, 2011
Singapore	51.24	7.06	ND	ND	12.28	16.61	--	ND	Cuong *et al.*, 2005.
Panama	10.90	4.90	294.0	199.9	38.00	13.70	--	ND	Guzmán & Jiménez, 1992
USEPA	> 200	> 50	> 500	> 50	> 60	> 50	--	--	Beyer, 1990

In general, nearly trace element levels in mangrove sediment in the studied areas were slightly higher than those from the coastal areas in China **(Qiu *et al.*, 2011)**, the coastal areas of the Red sea, Egypt **(El-Said & Youssef, 2013)**, the coastal areas of the Arabian Gulf **(Alharbi & El-Sorogy, 2017)** and the Red Sea, Saudi Arabia **(Alzaharani *et al.*, 2018)**. These were considerably lower than those from UCC, EPA according to **Beyer (1990)**. There is some indication of Hg concentration (0.65 to 1.20 µg g^{-1} with an average of 0.98 µg g^{-1}) in the sediment-mangrove system. However, it is much weaker than that for other trace metals. Sediment from the South Florida estuaries, USA (0.001-0.219g g^{-1}, with an average of 0.020 g g^{-1}; **(Shi *et al.*, 2004)**) and the South China coast (.0015 - 0.201g g^{-1}, with an average value of 0.054 g g^{-1}; **(Qiu *et al.*, 2011)**) had significantly lower Hg contents (2010). In general, our findings indicate that, the origins of this metal can be traced back to human activity, such as the oil shipping harbor, electric generation, or the cement industry.

Ecological assessments

Geo-accumulation Index (I_{geo})

Zn, Cu, Mn, Ni, Pb, Cr, and Co were all found to have I_{geo} values below 0, indicating that they were undetectable in any studied sites (Table 4).

While only I_{geo} value of Hg can be classified as class II ($0 < I_{geo} < 1$) in all studied sites, which can be reflected as unpolluted to moderately contaminated sediments. This result may be attributed to refining deposits and untreated sewage effluents (Usman *et al.*, 2013), and urban development of electric and desalination plants, Petro Rabigh plant, and commercial harbors that stretch along the Red Sea shorelines may be accountable for the augmented concentrations of trace elements in the mangrove-sediment ecosystem (Badr *et al.*, 2009; Alzahrani *et al.*, 2018).

Table 4. Averages of a geo-accumulation index (*Igeo*) of the measured heavy metals in mangrove sediments for all investigated locations.

Locations	Averages of Geo-accumulation index (*Igeo*)							
	Zn	**Cu**	**Mn**	**Ni**	**Pb**	**Cr**	**Co**	**Hg**
Duba	-1.84UC	-0.83UC	-1.97UC	-1.75UC	-2.61UC	-1.21UC	-1.06UC	0.93UMC
Yanbu	-2.08UC	-1.17UC	-2.50UC	-2.28UC	-2.58UC	-1.55UC	-1.51UC	0.98UMC
Masturah	-2.27UC	-1.73UC	-1.86UC	-2.42UC	-1.58UC	-1.58UC	-1.82UC	0.49UMC
Rabigh-II	-0.76UC	-0.39UC	-1.36UC	-0.60UC	-2.87UC	-0.86UC	-0.06UC	0.87UMC
Rabigh-I	-2.86UC	-1.91UC	-2.90UC	-2.31UC	-2.30UC	-2.17UC	-2.03UC	0.57UMC
Thuwal	-1.59UC	-0.37UC	-2.08UC	-0.76UC	-2.09UC	-0.81UC	-0.78UC	0.20UMC
Zahban	-2.25UC	-1.99UC	-3.89UC	-2.42UC	-2.56UC	-1.37UC	-4.00UC	1.74MC
Jedahh	-2.27UC	-2.10UC	-3.53UC	-2.18UC	-2.32UC	-2.22UC	-1.99UC	0.86UMC
Almazilif	-2.09UC	-1.51UC	-2.86UC	-2.28UC	-2.88UC	-1.55UC	-1.54UC	0.75UMC
Al-Birk	-1.62UC	-1.24UC	-1.90UC	-2.12UC	-1.82UC	-1.25UC	-1.30UC	-0.42 UC
Average	**-1.96**	**-1.32**	**-2.49**	**-1.91**	**-2.36**	**-1.46**	**-1.61**	**0.70**
Min.	-2.86	-2.10	-3.89	-2.42	-2.88	-2.22	-4.00	-0.42
Max.	-0.76	-0.37	-1.36	-0.60	-1.58	-0.81	-0.06	1.74

Contamination factor (C_f) indices

Table 5 shows that, the lowest levels of contamination (C_f values) for Zn, Cu, Ni, Cr, and Co (all $C_f < 1$), while the highest levels of contamination were found for Cu and Ni (1 Cf =1 $\leq C_f < 3$). In contrast, Mn concentrations varied widely from mild (1.91; Zahban) to highly contaminated (11; Rabigh-II).

The highest C_f concentrations of Pb and Hg in the environment were found in the Rabigh-II site, at 24.76 and 68.53 Cf, respectively. In disparity, the lowermost concentrations of these metals were found in the Zahban site, at 4.29 and 4.45, respectively. In addition, Table 5 displays that 10% of all sites were contaminated to a moderate degree ($14 \leq Cd < 28$), and 90% of all sites were severely contaminated, as determined by the current study's standards. The pollutant load index ranged from 0.81 (in Zahban) to 2.75 (Rabigh-II). Rabigh-II (PLI = 2.75) and Thuwal Island (PLI = 2.26) were found to have the highest trace elements among the sites studied.

Table 5. Contamination factor, contamination factor degree, and pollution load index of trace elements in surface sediments in the study area.

Locations	Contamination factor								CF Degree	PL Index
	Zn	Cu	Mn	Ni	Pb	Cr	Co	Hg		
Duba	0.42	0.84	7.25	0.86	16.32	0.34	0.26	34.25	60.53	1.79
Yanbu	0.35	0.67	5.00	0.68	11.26	0.23	0.26	24.95	43.41	1.39
Masturah	0.31	0.45	7.79	0.66	17.52	0.21	0.53	20.23	47.70	1.52
Rabigh-II	0.89	1.14	11.00	1.09	24.76	0.75	0.22	68.53	108.37	2.75
Rabigh-I	0.21	0.40	3.79	0.44	8.52	0.23	0.32	17.43	31.33	1.05
Thuwal	0.50	1.16	6.69	1.13	15.05	0.67	0.37	41.58	67.15	2.26
Zahban	0.32	0.38	1.91	0.77	4.29	0.21	0.27	4.45	12.59	0.81
Jeddah	0.31	0.35	2.45	0.43	5.52	0.25	0.32	17.98	27.59	0.99
Almazilif	0.35	0.53	3.90	0.68	8.78	0.23	0.21	24.50	39.18	1.23
Al-Birk	0.49	0.64	7.59	0.83	17.07	0.26	0.45	28.98	56.30	1.81
Average	**0.41**	**0.66**	**5.74**	**0.76**	**12.91**	**0.34**	**0.32**	**28.29**	**56.30**	**1.81**
Min.	**0.21**	**0.35**	**1.91**	**0.43**	**4.29**	**0.21**	**0.21**	**4.45**	**39.18**	**1.23**
Max.	**0.89**	**1.16**	**11.00**	**1.13**	**24.76**	**0.75**	**0.53**	**68.53**	**27.59**	**0.99**

Potential Ecological Risk Indices (E_r^i) and Potential Toxicity Response Index (RI):-

Table 6 shows that the ecological risk assessment index (E_r^i) similarly correlates with the Igeo index. Zinc, copper, manganese, chromium, and cobalt all showed low ecological risk in all sediments (E_r^i< 40). Conversely, Ni showed substantial risk ($80 \le E_r^i < 160$), and Hg showed significant risk ($160 \le E_r^i < 320$) at all study sites. The Pb ecological risk assessment index (E_r^i) ranged from 21.45 in the Zahban to 123.80 in the Rabigh-II sites. This may result from untreated sewage effluents and the enormous quantities of anthropogenic wastes produced by industrial processes like refining (Usman *et al.*, 2013; Alzahrani *et al.*, 2018; Alharbi *et al.*, 2019). Regarding *RI* value, Zahban had the lowest value (300.3), and Rabigh-II had the highest (2890.4), with an average of 1302.6. There was a 10% split between the moderate risk group (*RI* ranges, $150 \le RI < 300$) and the substantial risk category ($300 \le RI < 600$).

Table 6. Potential ecological risk indices (E_r^i) and potential toxicity response index (*RI*) of trace elements under the study area.

Locations	**Ecological risk categories of single heavy metal (E_r^i)**								***RI Value***
	Zn	**Cu**	**Mn**	**Ni**	**pb**	**Cr**	**Co**	**Hg**	
Duba	0.42/LR	4.22/LR	7.25/LR	4.30/LR	81.58/CR	0.67/LR	1.29/LR	1370/VHR	1469.7/VHR
Yanbu	0.35/LR	3.34/LR	5.00/LR	3.40/LR	56.28/MR	0.47/LR	1.32/LR	998/VHR	1068.2/VHR
Masturah	0.31/LR	2.26/LR	7.79/LR	3.32/LR	87.61/CR	0.42/LR	2.64/LR	809/VHR	913.4/VHR
Rabigh-II	0.89/LR	5.72/LR	11.00/LR	5.46/LR	123.80/CR	1.49/LR	1.08/LR	2741/VHR	2890.4/VHR
Rabigh-I	0.21/LR	1.99/LR	3.79/LR	2.21/LR	42.62/MR	0.46/LR	1.60/LR	697/VHR	749.9/VHR
Thuwal	0.50/LR	5.80/LR	6.69/LR	5.65/LR	75.26/MR	1.34/LR	1.86/LR	1663/VHR	1760.1/VHR
Zahban	0.32/LR	1.89/LR	1.91/LR	3.85/LR	21.45/LR	0.42/LR	1.34/LR	178/HR	209.2/MR
Jeddah	0.31/LR	1.75/LR	2.45/LR	2.13/LR	27.58/LR	0.50/LR	1.58/LR	719/VHR	755.3/VHR
Almazilif	0.35/LR	2.64/LR	3.90/LR	3.38/LR	43.89/MR	0.47/LR	1.07/LR	980/VHR	1035.7/VHR
Al-Birk	0.49/LR	3.18/LR	7.59/LR	4.17/LR	85.35/CR	0.52/LR	2.24/LR	1159/VHR	1262.5/VHR
Average	**0.41/LR**	**3.28/LR**	**5.74/LR**	**3.80/LR**	**64.54/MR**	**0.68/LR**	**1.60/LR**	**1131.4/VHR**	**1302.6/VHR**
Min.	0.21	1.75	1.91	2.13	21.45	0.42	1.07	178	300.32
Max.	0.89	5.8	11	5.65	123.8	1.49	2.64	2741	2979.98

Trace metal contents in mangrove plants (leaves and roots):-

A. marina leaves and roots contain significantly different amounts of trace metal, as illustrated in Fig. 4. The following is a list of the trace metals found in leaves, in the order in which they are found, Mn (47.65 ± 4.21) > Cr (15.57 ± 0.95) > Cu (10.65 ±1.10) > Zn (10.47± 0.75) > Ni (8.95 ± 0.70) > Pb (3.78 ± 0.49) > Co (0.84 ± 0.06) > Hg (0.14 ± 0.03), respectively. The following is a list of the average concentrations of trace metals in root tissues, from highest to lowest: 22.25 ± 2.56 > 10.02 ± 0.59 > 7.55 ± 0.87 > 7.31 ± 0.78 > 6.27 ± 0.69 > 1.74 ± 0.28 > 1.04 ± 0.05 > 0.23 ± 0.03 for Mn, Cr, Ni, Cu, Zn, Pb, Co, and Hg, respectively. Mainly, Mn levels in mangrove tissues were much higher than in the other trace metals studied.

Concentrations of Zn in the leaves ranged from 7.88 at Rabigh II to 14.41 µg g^{-1} in Duba (Fig. 4). Cu concentrations varied between 7.51 and 20.23 µg g^{-1} at Yanbu and Al-Birk, respectively. Mn concentrations varied from 28.85 µg g^{-1} in Zahban to 70.23 µg g^{-1} at Al-Birk. While Ni concentrations ranged from 5.09 µg g^{-1} at the Almazilif site to 12.9 µg g^{-1} at the Rabigh-II site, Co concentrations were very consistent across all sites. Leaf Pb concentrations in mangrove trees varied from 1.87 µg g^{-1} at Almazilif to 5.89 µg g^{-1} at Masturah. On the other hand, the concentration of Cr metal increased from 10.1 µg g^{-1} at Jeddah to 19.08 µg g^{-1} on Thuwal Island. In addition, Co concentrations differed from 0.63 g g-1 at the Almazilif location to 1.02 g g-1 at the same site. Last but not least, the Hg concentrations varied from 0.06 µg g^{-1} in Jeddah to 0.35 µg g^{-1} on Thuwal.

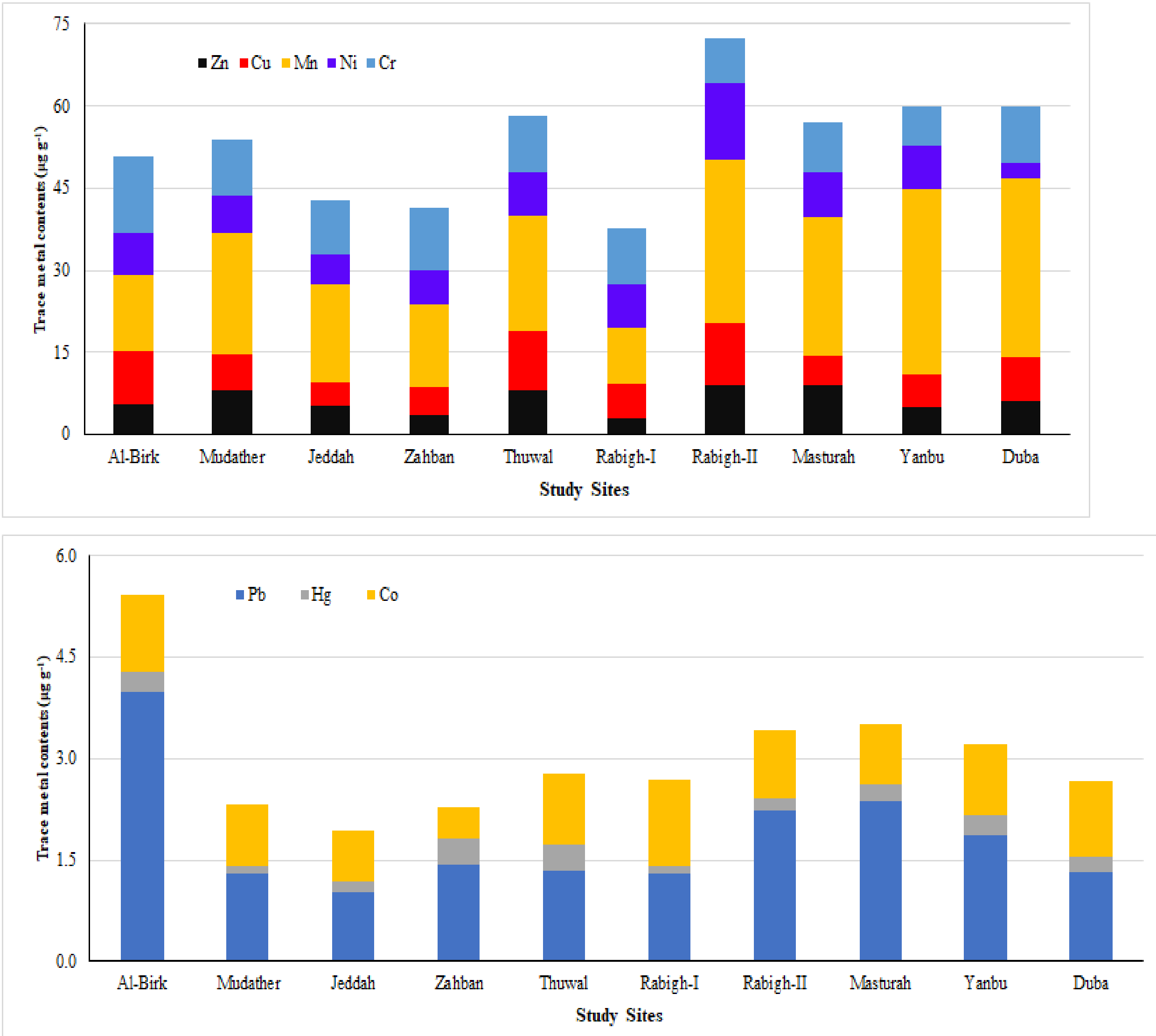

Fig. 4. Cumulative figure of Trace metal contents (µg g^{-1} DW) in mangrove root along Study sites.

However, as seen in Fig. 5, the highest concentrations of Zn, Cu, Mn, Ni, pb, Cr, Co, and Hg were 6.27, 7.31, 22.25, 7.55, 1.82, 10.02, 0.96, and 0.23 µg g^{-1}, respectively, in the roots. In most cases, leaf concentrations were higher than root concentrations for these metal ions. Mn introduced substantially higher amounts suggesting its role as a necessary micronutrient that supports multiple enzyme activities, even though most trace elements collected in mangrove leaf and root tissues were lower than those in the relevant sediments (Ernst *et al.*, 1992).

Some trace elements, like Zn, Mn, Ni, and Co, were found to be significantly higher within the surface sediments in Rabigh-II, which may be attributable to industrial activity. This was shown to be the case for both the leaves and roots of mangrove trees.

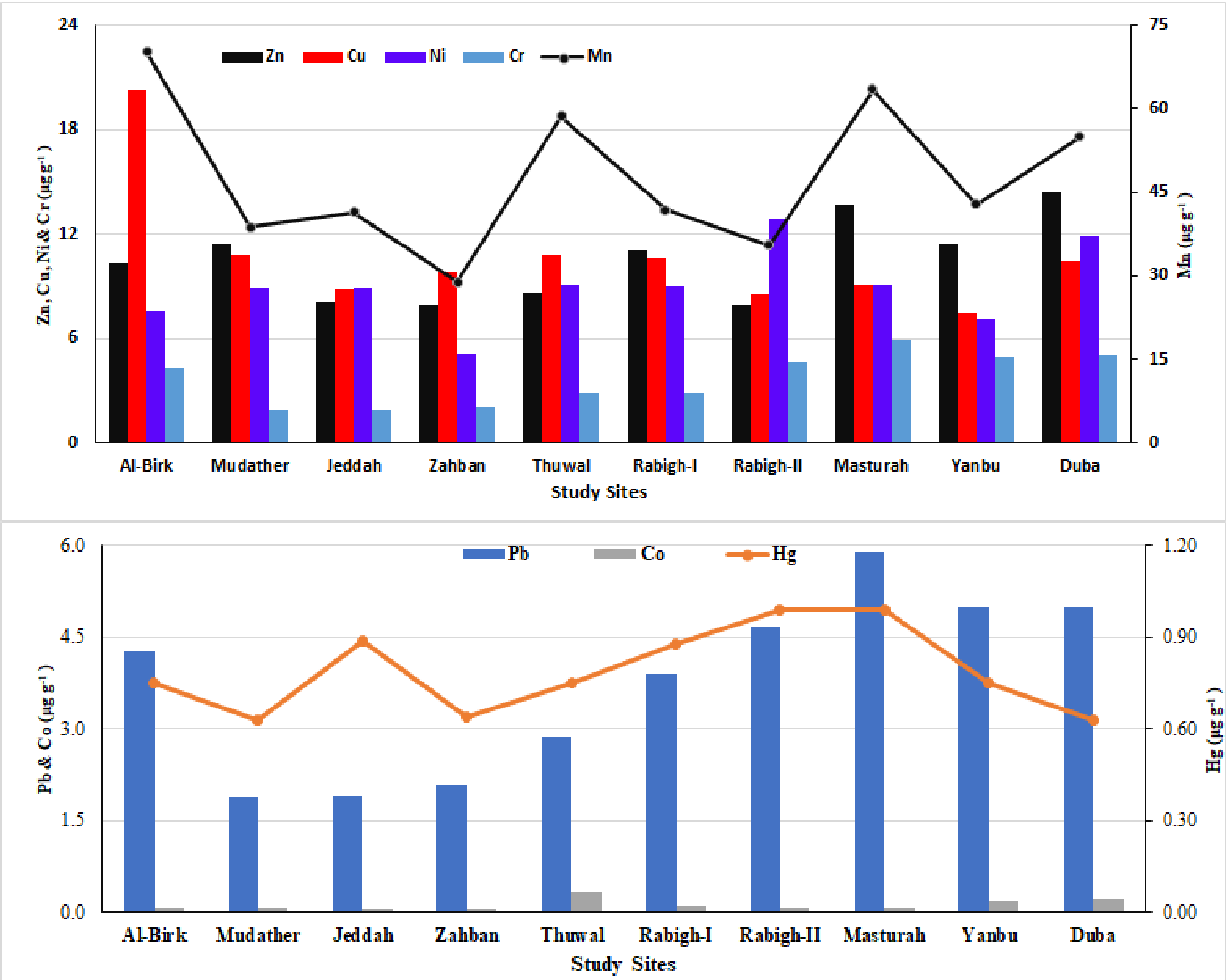

Fig 5. Cumulative figureof heavy metals concentrations (µg g^{-1}) in leaf of the grey mangrove ecosystem study sites.

Biological Accumulation Factor (BAFs):

In the current investigation, it observed that the descending averages of BAFs for mangrove leaves followed the order of Pb (0.61) > Cu (0.44) > Ni (0.33) > Cr (0.32) > Zn (0.31) > Mn (0.22) > Hg (0.15) > Co (0.11) while, BAFs averages for roots were Pb (0.31) > Ni (0.29) > Cu (0.26) > Hg (0.24) > Cr (0.21) > Zn (0.17) > Co (0.11) > Mn (0.10) respectively.

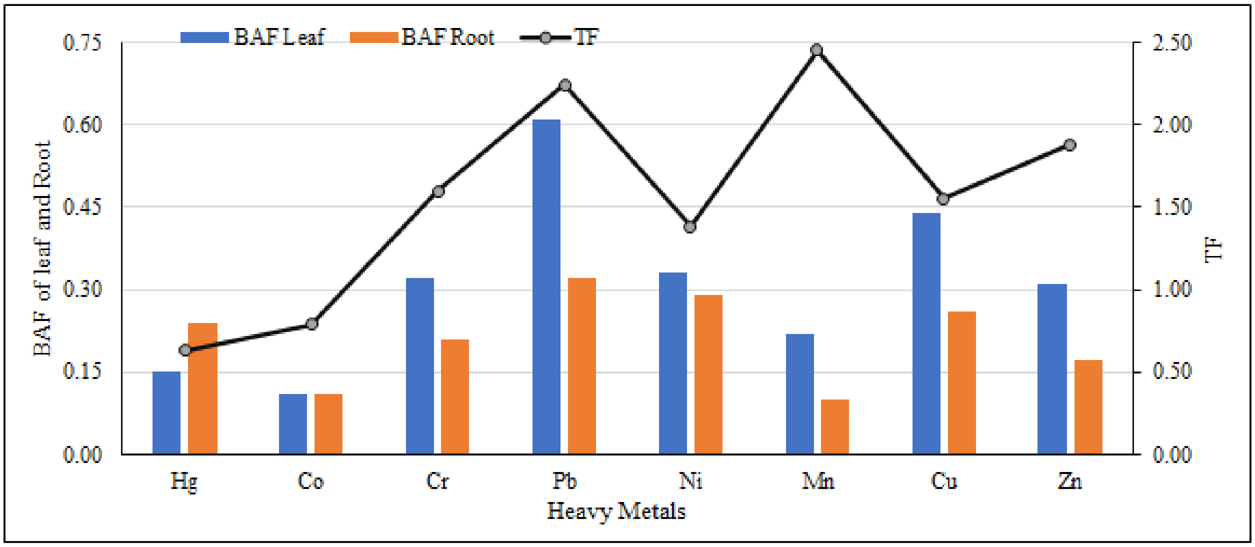

Fig 6. Bioaccumulation factor (BAFs), indicating the ratio of the average metal concentrations in leaf and root tissues to sediment over all study sites.

Finally, Pb is stored in mangrove leaf and root tissues, as they had the highest BAF values (0.61 for Pb in lead and 0.31 for root) for the area under investigation. The records acquired showed that the maximum BAFs value of Pb was 1.14 with mangrove leaf tissues at Rabigh II and 1.02 with mangrove leaf tissues at Duba, permitting symptoms of critical pollution (BAFs >1 represented high accumulated metals in leaf and root tissues). Additionally, the values obtained for BAFs with leaves were higher than those for BAFs with roots. Immobilization processing for metals due to complexation with organic components may account for the low acceleration of trace metals like Hg in the sediment-mangrove ecosystem, as shown by the lowest BAF values in the very severely contaminated sediments in Table (5). (Nath *et al.*, 2014). Consequently, there needs to be a greater emphasis on understanding the adsorption and acceleration of trace metals in sediment-mangrove environments during the speciation processes of these elements (Luo *et al.*, 2017). Plants with TF values more than 1 are considered hyperaccumulators for metals in polluted sediments, as stated by Srivastava *et al.* (2006). The recorded metals' TF values followed the pattern indicated in Fig. (6), Mn (2.45) > Pb (2.24) > Zn (1.88) > Cr (1.60) > Cu (1.55) > Ni (1.38) > Co (0.79) > Hg (0.63). Except for the metals Co and Hg, these results show that all TF averages are significantly more than 1. Mn (47.67 µg g^{-1} DW), Pb (3.74 µg g^{-1} DW), Zn (10.50 µg g^{-1} DW), Cr (15.59 µg g^{-1} DW), Cu (10.67 µg g^{-1} DW) and Ni (8.59 µg g^{-1} DW), respectively, all had significantly higher average concentrations, lending credence to this result. Many of the shorelines in Saudi Arabia have introduced new forms of pollution as a result of human activities including industry and tourism, as shown in the current study (Badr *et al.*, 2009; Alzahrani *et al.*, 2018; Almahasheer *et al.*, 2018 and Alharbi *et al.*, 2019).

Pearson's correlation analysis

Pearson's correlation were presented to calculate the inter-connection between the contaminants and physico-chemical properties of the mangrove sediments (Table 7).

Table 7. Pearson correlation coefficients among soil properties and trace elements concentration

	Sand %	**Mud %**	**pH**	**EC**	**$CaCO^-_3$**	**SOC %**	**Zn**	**Cu**	**Mn**	**Ni**	**Pb**	**Cr**	**Co**
Mud	**-1.00**												
pH	0.244	-0.244											
EC	0.320	-0.320	0.154										
$CaCO^-_3$	-0.009	0.009	-0.019	0.357									
SOC %	0.182	-0.182	0.385	0.416	0.124	1.00							
Heavy metals in sediments													
Zn	-0.429	0.429	-0.254	-0.254	-0.231	-0.089							
Cu	-0.463	0.463	0.205	-0.209	-0.195	0.144	**0.807**						
Mn	-0.298	0.298	0.107	-0.129	-0.239	0.414	**0.793**	**0.739**					
Ni	-0.361	0.361	0.027	-0.232	-0.002	0.064	**0.847**	**0.916**	**0.656**				
Pb	**0.666**	**-0.666**	0.331	0.237	-0.204	0.725	-0.242	-0.190	0.199	-0.207			
Cr	-0.237	0.237	0.060	0.049	-0.213	0.147	**0.789**	**0.900**	**0.638**	**0.818**	-0.083		
Co	-0.539	0.539	0.038	-0.338	-0.142	0.042	**0.924**	**0.891**	**0.848**	**0.889**	-0.226	**0.732**	
Hg	-0.107	0.107	**-0.612**	0.322	0.256	-0.363	-0.143	-0.284	-0.480	-0.195	-0.541	-0.107	-0.355

Bold numbers observed a significant correlation ($p < 0.05$).

The results of this research showed poor trace element absorption in coarse-grained sediment was caused by a combination of factors, such as weathering, hydrodynamic movement, and the deposition mechanism of fine-grained sediment. All trace elements, except for Pb, were shown to have a strong negative relationship with the sand proportion of sediments. In other hand, all trace elements in the sediments excluding Pb were displayed to have statistically significant positive relations with the mud fraction. Fine-grained sediments have been found to accumulate Zn, Cu, Mn, Ni, Cr, Co, and Hg, suggesting that they may significantly transport these metals. High surface area, cation exchange capacity, and inorganic or organic deposition could all play a role in this (Kumar *et al.*, 2016 and Rong *et al.*, 2022). No statistically significant associations were found between SOC and any of the trace elements in the sediments analyzed in this investigation. Therefore, the current study's OM content cannot play a definitive role in identifying the origin of trace elements. Yet, the geochemical behavior of trace metals in the marine environment is reflected in the strong link observed between organic matter and trace elements via adsorption and complexation action (Marchand *et al.*, 2011). In addition, there is a positive correlation between salinity and SOC, although a weak one (r = 0.416). High salinity, as reported by Van de Broek *et al.* (2016), reduces metabolic activity in the sediment-mangrove ecosystem, leading to a greater buildup of organic matter.

Principal component analysis (PCA):-

Principal component analysis (PCA) and Eigenvalues performed a considerable role in the current study in determining the connections of heavy metals with Metallo-organic compounds (chelation) and in understanding the circumstances of sediment. Moreover, PCA rotation was executed using the Varimax technique. Table 8 emphasizes the significance of loadings greater than 0.60.

Table 8. Varimax rotated principal component analysis (PCA) of measured heavy metals in sediment samples (bold loadings are statistically significant).

Studied variables	**Factor 1**	**Factor 2**	**Factor 3**	**Factor 4**
Ni-sedm.	**.943**			
Cr-sedm.	**.927**			
Cu-sedm.	**.926**	.222		.246
Zn-sedm.	**.917**	.170		-.276
Co-sedm.	**.903**	.288		
Mn-sedm.	**.785**	.129	.491	
Sand%	-.290	**-.929**		
Mud%	.290	**.929**		
Hg-sedm.	-.228	**.617**	-.454	-.401
SOC%			**.901**	.208
Pb-sedm.	-.119	-.605	**.753**	
pH		-.154	.197	**.951**
EC	-.118	-.161	.194	
CaCO3%	-.123			
Eigenvalue	5.818	3.497	1.468	1.016
Variance %	41.559	24.976	10.489	7.254
Cumulative %	41.559	66.535	77.024	84.90

Four variables were identified in the factorial analysis of mangrove sediments, accounting for 84.90%. A total of 41.56% of the variation was explained by the first dominating factor, which had an Eigenvalue of 5.82. In this context, "heavy metals" refer to elements such as Cu, Ni, Cr, Zn, Co, and Mn that build up in the environment. This confirms what has been found in prior studies throughout the Red Sea coast by researchers including Badr *et al.* (2009), Alzahrani *et al.* (2018), Almahasheer *et al.* (2018), Alharbi *et al.* (2019) and Ouma *et al.*, (2022). Significant loading was found for Sand%, Mud%, and Hg-sedm on the second factor, which accounted for 24.98% of the total variance and had an Eigenvalue of 3.50. Human activities, such as bridge construction, may be to blame for the current situation, as they have cut off most mangrove regions from the open sea. The third factor (10.49% of total variance; Eigenvalue = 1.47). This component heavily influenced both SOC% and Pb-sedim. Finally, the load on pH was carried by the fourth component, which explained 7.26% of the overall variation (Eigenvalue = 1.02).

CONCLUSION

The results showed that the sediment-mangrove ecosystems along the Red Sea coast are vulnerable to introducing potentially hazardous materials. The results of the present study suggest that PTE levels in mangrove sediments in these lagoons are relatively high, posing an unnecessary risk to marine ecosystems at the Rabigh-II, Thuwal Island, and Yanbu sites. Anthropogenic causes such as urbanization, fossil fuel extraction, petrochemical processing, wastewater treatment plants, and desalination facilities pose a significant threat to mangrove ecosystems in the study areas. These findings may improve our understanding of how sediment pollution in forests changes in response to climatic, industrial, and societal factors.

Further, the results can be applied to developing a decision-making framework for the sustainable management of Saudi Arabia's natural aquatic ecosystems, particularly along the Red Sea's shorelines, to incorporate cutting-edge business practices and a representative, long-term approach to the care of these areas. To better understand the adsorption and acceleration of trace elements, as well as the quantity of these metals in sediment and various organs of mangrove plants, more attention needs to be paid to the speciation processing of trace elements in sediment-mangrove.

REFERENCES

Abohassan, R. A. (2013). Heavy metal pollution in *Avicennia marina* mangrove systems on the Red Sea Coast of Saudi Arabia. JKAU: Meteorology, Environment and Arid Land Agriculture Sciences **24**(1):35 -53.

Alharbi, O. M.; L. Rafat A.; Khattab, Imran A.; Yaser S. and Binnaser, Adnan Aqeel (2019). Assessment of heavy metals contamination in the sediments and mangroves (*Avicennia marina*) at Yanbu coast, Red Sea, Saudi Arabia. Marine Pollution Bulletin, **149**, 110669. https://doi.org/10.1016/j.marpolbul.2019.110669.

Alharbi, Talal; El-Sorogy, Abdelbaset (2017). Assessment of metal contamination in coastal sediments of Al-Khobar area, Arabian Gulf, Saudi Arabia. Journal of African Earth Sciences, **129**., 458–468. doi: 10.1016/j.jafrearsci.2017.02.007

Al-Hasawi, Z.M.; Hariri, M.S. and Touliabah, H.E. (2022). Physico-chemical factors and biodiversity of microalgal flora in Rabigh Lagoon under Global Climate Change." Fresenius Environmental Bulletin **31**(8): 7646-7658.

Almahasheer H., Carlos M. Duarte and Xabier I. (2018). Leaf Nutrient Resorption and Export Fluxes of *Avicennia marina* in the Central Red Sea Area Frontiers in Marine Science. Volume 5 Article 204 www.frontiersin.org.

Almahasheer H.; Oscar S.; Carlos M. D. and Xabier I. (2016). Remobilization of Heavy Metals by Mangrove Leaves. Frontiers in Marine Science. Volume **5**: 484. www.frontiersin.org

Alzahrani, D. A.; Selim, E. M. and El-Sherbiny, M. M. (2018). Ecological assessment of heavy metals in the grey mangrove (*Avicennia marina*) and associated sediments along the Red Sea coast of Saudi Arabia. Oceanologia, **60**: 513-526.

Badr, N. B. E.; El-Fiky, A. A.; Mostafa, A. R. and Al-Mur, B. A. (2009). Metal pollution records in core sediments of some Red Sea coastal areas, Kingdom of Saudi Arabia. Environ. Monit. Assess. **155** (1), 509— 526, http://dx.doi.org/10.1007/s10661-008-0452-x.

Bakshi, M.; Ghosh, S.; Chakraborty, D.; Hazra, S. and Chaudhuri, P., (2018). Assessment of potentially toxic metal (PTM) pollution in mangrove habitats using biochemical markers: A case study on *Avicennia officinalis* L. in and around Sundarban, India.Mar. Pollut. Bull. **133**: 157-172.

Bettinelli, M., G. M. Beone, S. Spezia and C. Baffi (2000). Determination of heavy metals in soils and sediments by microwave-assisted digestion and inductively coupled plasma optical emission spectrometry analysis." Analytica Chimica Acta **424**: 289-296.

Beyer W. N. (1990). Evaluating soil contamination. Fish and Wildlife Service, Washington, DC.

Cuong D.T. S.; Bayen, O.; Wurl, K.; Subramanian, K. K. S.; Wong, N.; and Sivasothi, J. P. Obbard (2005). Heavy metal contamination in mangrove habitats of Singapore, Mar. Pollut. Bull. **50**: 1713–1744.

Dane, J. H., and Topp, C. G. (2020). Methods of Soil Analysis, Part 4: Physical Methods. John Wiley & Sons.

El-Juhany LI. (2009). Present status and degradation trends of mangrove forests on the southern Red Sea coast of Saudi Arabia. Am Euras J Agric Environ Sci.; **6**:328–340.

El-Said, G. F. and Youssef, D. H. (2013). Ecotoxicological impact assessment of some heavy metals and their distribution in some fractions of mangrove sediments from Red Sea, Egypt. Environ. Monit. Assess., **185** (1): 393 - 404

El-Said, G. F. and Youssef, D. H. (2013). Ecotoxicological impact assessment of some heavy metals and their distribution in some frac-tions of mangrove sediments from Red Sea, Egypt. Environmental Monitoring Assessment, **185**(1), 393–404. https://doi.org/10.1007/s10661-012- 2561-9.

Ernst W. H. O.; Verkleij J. A. C. and Schat H. (1992). Metal tolerance in plants, Acta Botanica Neerlandica, **41**: 229-248.:https://doi.org/10.1111/j.1438-8677.1992. tb01332.x.

Guzmán, H. M. and Jiménez, C. E., (1992). Contamination of coral reefs by heavy metals along the Caribbean coast of Central America (Costa Rica and Panama). Mar. Pollut. Bull. **24** (11): 554—561, http://dx. doi.org/10.1016/0025-326X (92)90708-E.

Håkanson L., (1980). Ecological risk index for aquatic pollution control. A sedimentological approach, Water Research, **14**(8), 975-1001.

Jackson, M. L. (2005). Soil chemical analysis: advanced course. UW-Madison Libraries Parallel Press.

Jiang R.; Huang S.; Wang W.; Liu Y.; Pan Z.; Sun X.; Lin C. (2020). Heavy metal pollution and ecological risk assessment in the Maowei sea mangrove, China. Mar. Pollut. Bull. **161**: 111816 10.1016/j.marpolbul.2020.111816.

Kiymaz, S. U.; Karadavut, A.; Makalesi and Yazar S. (2014). Tarım Bilimleri Dergisi Application of Multivariate Statistical Analysis in the Assessment of Surface Water Quality in Seyfe Lake, Turkey Türkiye'de Seyfe Gölü Yüzey Su Kalitesinin Değerlendirilmesinde Çok Değişkenli İstatistiksel Analizlerin Uygulanması ESER BİLGİSİ."

Kristensen E.; Bouillon S.; Dittmar T. and Marchand C. (2008). Organic carbon dynamics in mangrove ecosystems: A review. Aquatic Botany. **89**: 201-219. doi: 10.1016/j.aquabot.2007.12.005.

Kumar A.; Ramanathan A. L.; Prasad M. B. K.; Datta D.; Kumar M. and Sappal S. M. (2016) Distribution, enrichment, and potential toxicity of trace metals in the surface sediments of Sundarban mangrove ecosystem, Bangladesh: a baseline study before Sundarban oil spill of December, Environmental Science and Pollution Research, **23**(9): 8985-8999. doi:10.1007/s11356-016-6086-6.

Kumar, A. (2017). Environmental degradation along the Persian/Arabian Gulf Coast of Saudi Arabia." E Journal Earth Science India **10**: 1-13.

Luo X.; Yu L.; Wang C.; Yin X.; Mosa A. and Lv J. (2017). Sorption of vanadium (V) onto natural soil colloids under various solution pH and ionic strength conditions. Chemosphere Feb; **169**:609–17

Marchand C.; Allenbach M.; Lallier-Vergès E. (2011). Relationships between heavy metals distribution and organic matter cycling in mangrove sediments (Conception Bay, New Caledonia). Geoderma, **160**(3- 4), 444 - 456.

Mosa A.E.M.; Selim Sh. M.; El-Kadi A. A.; Khedr, A. A.; Elnaggar, W. A.; Hefny, A. S.; Abdelhamid, A. M.; El Kenawy, A. E. H.; Wang, S. and Shaheen M. (2022). Ecotoxicological assessment of toxic elements contamination in mangrove ecosystem along the Red Sea coast, Egypt. Bulletin Marine Pollution Bulletin **176** :113446.

Muangthong, S. (2015). Assessment ecosystem of the Lamtakong River Basin (Thailand) using multivariate statistical techniques. 4**.**

Mustapha, A. and A. Z. Aris (2012). Multivariate Statistical Analysis and Environmental Modeling of Heavy Metals Pollution by Industries." Polish Journal of Environmental Studies **21**: 1359-1367.

Mustapha, A., A. Z.; Aris, M. Ramli and H. Juahir (2012). Spatial-temporal variation of surface water quality in the downstream region of the Jakara River, north-western Nigeria: A statistical approach." Journal of environmental science and health. Part A, Toxic/hazardous substances & environmental engineering **47**: 1551-1560.

Müller, G., (1969). Index of geoaccumulation in sediments of the Rhine River. Geo J. **2** (3): 108 -118.

Nath B, Birch G, Chaudhuri P. (2014). Assessment of sediment quality in *Avicennia marina*-dominated embayment of Sydney Estuary: the potential use of pneumatophores (aerial roots) as a bio-indicator of trace metal contamination, Science of the Total Environment. **472**:1010-22. 10.1016/j. scitotenv.2013.11.096.

Ouma, K.; A. Shane and S. Syampungani (2022). Aquatic Ecological Risk of Heavy-Metal Pollution Associated with Degraded Mining Landscapes of the Southern Africa River Basins: A Review. Minerals **12**: 225.

Piper, C. S. (2017). Soil and Plant Analysis. Scientific Publishers.

Qi-juan C.; Zi-yao Z.; Ying-wen L.; Xiao-hui W. and Zeng-hui H. (2021). Community Characteristics of a Mangrove Area in Zhanjiang and Its Relationship with Topsoil Pollen Assemblage. Geogr. Sci. Res, **10**: 64–71.

Qiu, Y. W.; Yu, K. F.; Zhang, G. and Wang, W. X. (2011). Accumulation and partitioning of seven trace metals in mangroves and sediment cores from three estuarine wetlands of Hainan Island, China. J. Hazard. Mater., **190**(1-3): 631-638.

Rogers K. G.; Goodbred S. L. J. and Mondal D. R. (2013). Monsoon sedimentation on the 'abandoned' tide-influenced Ganges-Brahmaputra delta plain Estuarine, Coastal and Shelf Science, , **131**: 297-309. doi: 10.1016/j.ecss.2013.07.014.

Rong, S., J. Wu, X. Cao and Y. Sun (2022). Comprehensive Ecological Risk Assessment of Heavy Metals Based on Species Sensitivity Distribution in Aquatic of Coastal Areas in Hong Kong. Int J Environ Res Public Health **19**(20).

Sanders C. J.; Santos I. R.; Barcellos R.; Silva Filho E.V. (2012). Elevated concentrations of dissolved Ba, Fe and Mn in a mangrove subterranean estuary: consequence of sea level rise. Continental Shelf Research, **43**: 86-94.

Sarker S.; Masud-Ul-Alam M. and Hossain M. S. (2021). Rahman Chowdhury S.; Sharifuzzaman S. M. A review of bioturbation and sediment organic geochemistry in mangroves. Geol. J., **56**: 2439–2450. 10.1002/gj.3808.

Sparks, D. L.; Page, A. L.; Helmke, P. A. and Loeppert, R. H. (2020). Methods of Soil Analysis, Part 3: Chemical Methods. John Wiley & Sons.

Spencer K. L.; Cundy A. B. and Croudace I. W. (2003). Heavy metal distribution and early diagenesis in salt marsh sediments from the Medway Estuary, Kent, UK. Estuarine, Coastal and Shelf Science, , **57**(1-2): 43–54.

Srivastava, M.; Ma, L. Q. and Santos, J. A. G. (2006). Three new arsenic hyperaccumulating ferns. Sci. Total Environ. **364**: 24 –31.

Taylor, S. R. and McLennan, S. M. (1985). The Continental Crust: Its Composition and Evolution. Blackwell, London.

Tokatli C. (2019). Sediment quality of Ergene River basin: bio–ecological risk assessment of toxic metals. Environ Monit Assess. **191**:706–717.

Turekian, K. K. and Wedepohl, K. H. (1961). Distribution of the elements in some major units of the earth's crust. Geol. Soc. Am. Bull. **72**(2): 175—192, http://dx.doi.org/10.1130/0016-7606(1961)72 [175.

Usman, A. R.; Alkredaa, R. S. and Al-Wabel, M. I. (2013). Heavy metal contamination in sediments and mangroves from the coast of Red Sea: *Avicennia marina* as potential metal bioaccumulator. Ecotoxicol. Environ. Saf. **97**: 263-270, http://dx.doi.org/ 10.1016/j.ecoenv.2013.08.009.

Ustaoğlu F.; Tepe Y. and Aydin H. (2020). Heavy metals in sediments of two nearby streams from southeastern Black Sea coast: contamination and ecological risk assessment. Environ Forensics.**21**(2):145 -156.

Van de Broek, M.; Temmerman, S.; Merckx, R. and Govers, G., (2016). The importance of an estuarine salinity gradient on soil organic carbon stocks of tidal marshes. Biogeosci. Discuss., http://dx. doi.org/10.5194/bg-2016-285.

Walkley, A. and Black, I. A. (1934). An examination of the Degtareff method for determining soil organic matter, and a proposed modification of the chromic acid titration method. Soil Sci. **37**(1): 29 -38.

Yuan G. L.; Liu C.; Chen L. and Yang Z. (2011). Inputting history of heavy metals into the inland lake recorded in sediment profiles: Poyang Lake in China. J. Hazard. Mater. **185**:336–345.

Zhang, C.; Shan, B.; Tang, W.; Dong, L.; Zhang, W. and Pei, Y. (2017). Heavy metal concentrations and speciation in riverine sediments and the risks posed in three urban belts in the Haihe Basin. Ecotoxicol. Environ. Saf. **139**: 263–271.

Zhou, J. D.; Ma, J.; Pan, W.; Nie and K. Wu (2007). Application of multivariate statistical approach to identify heavy metal sources in sediment and waters: a case study in Yangzhong, China." Environmental Geology **54**(2): 373-380.